# Electronic Commutation Consideration in Modeling of Radial-Flux Surface Mounted PM Machines

**Payam Vahedi**

***Abstract*— In order to keep the permanent magnet motor running, the magnetic field produced by the windings should shift position, as the rotor moves to catch up with the stator field. Rotor position is sensed using Hall effects sensors. With these sensors 6 different commutation are possible every 15°. Hence, this paper presents a model procedure for these 6 points. The aim of this paper is presented a magnetic model of surface mounted permanent magnet machine for different rotor positions. This paper is presented a PM machine with double layer concentrated winding with 8 poles and 12 slots. The FEM analysis is used for validation of models.**

***Index Terms*— Finite element method, Modeling Permanent magnet machine, Radial flux**

## I. INTRODUCTION

Rotor position is sensed using three Hall effect sensors embedded into the stator. Whenever the rotor magnetic poles pass near the Hall sensors, they give a high or low signal, indicating the N or S pole is passing near the sensors. Based on the combination of these three Hall sensor signals, the exact sequence of commutation can be determined. To obtain the complete magnetic model, we should be determined winding energizing sequence with respect to the Hall sensor (Fig. 1). This paper is presented a PM machine with double layer concentrated winding with 8 poles and 12 slots. The parameters of machine are obtained from [1]. These values are given in table 1. In fig. 1, six statuses (A to F) have been introduced. The aim of this paper is presented magnetic model in these six statuses.

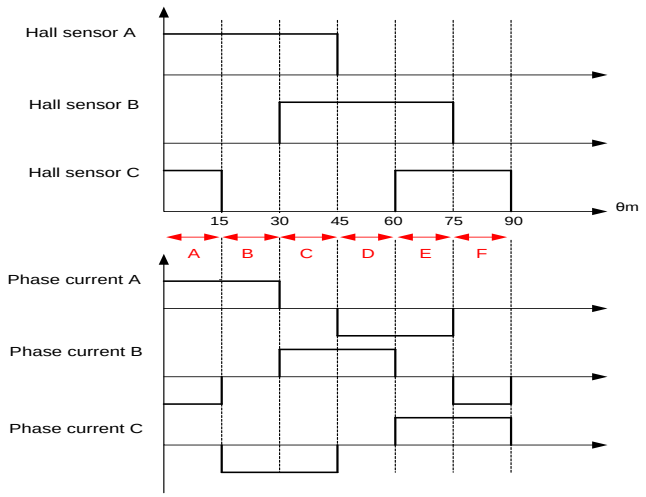


**Fig. 1 Winding Energizing Sequence with Respect to the Hall Sensor (Electronic Commutation)**

**Manuscript Received on August 2014.**

**Payam Vahedi**, He received the B.Sc. Degree in Electrical Engineering from Chamran University, Ahvaz, Iran.

**Table 1 Specifications of Machine**

| | |
|---|---|
| Stator outer diameter (m) | 0.1655 |
| Stator inner diameter (m) | 0.0778 |
| Number of poles | 8 |
| Number of slots | 12 |
| Magnet thickness (m) | 0.0124 |
| Tooth width (m) | 0.0077 |
| Height of the stator slot (m) | 0.03285 |
| Height of the stator wedge (m) | 0.003 |
| Height of the stator yoke (m) | 0.008 |
| Length of machine (m) | 0.165 |
| Shaft diameter (m) | 0.1655 |
| Half pole angle in electrical degrees | 60 |
| Current (A) | 10 |
| Output power (KW) | 5.5 |

Proposed magnetic model in this paper has some advantages compared to the magnetic model in [2] and [3]:
1- Considering the effect of rotation in magnetic model.
2- Considering the leakage flux between two poles.
3- The magnetic models cover all parts of the machine.

## II. MODELING OF MACHINE COMPONENT

Fig. 2 shows the simulation of radial flux surface mounted permanent magnet machine by finite element method (FEM). With regard to fig. 2 the machine component are modeled as follow:

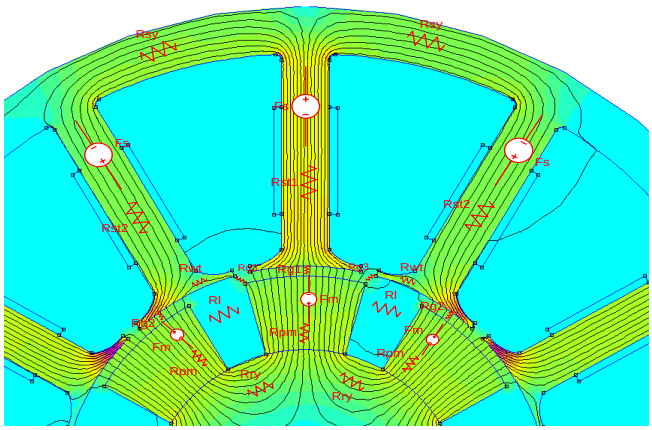

**Fig. 2 Simulation of SMPM Machine by Finite Element Method**

### *A. Rotor Modeling:*

In this paper, the equivalent magnetic circuit for permanent magnet (PM) is a source of magneto motive force (MMF) series with reluctance of the PM [5]. This model is shown in figure 3.



*Published By:*
*Blue Eyes Intelligence Engineering*
*& Sciences Publication Pvt. Ltd.*

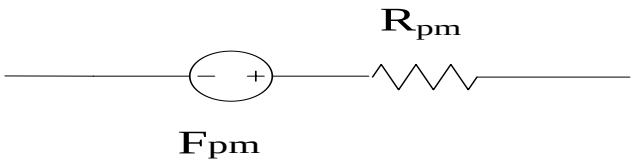


**Fig. 3 Modeling of Permanent Magnet**

Rotor yoke is modeled with nonlinear reluctance (Fig. 4).

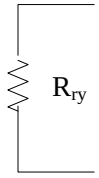


**Fig. 4 Modeling of Rotor Yoke**

***B. Stator modeling:***

Model of stator winding is the MMF of winding (Fig. 5).

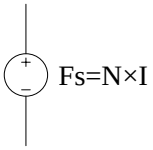


**Fig. 5 Modeling of Stator Winding**

Stator yoke, stator teeth and stator wedge are modeled with nonlinear reluctances (Fig. 6).

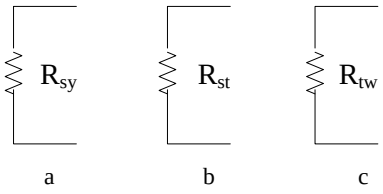


**Fig. 6 Modeling of A) Stator Yoke B) Stator Tooth c) Stator Wedge**

***C. Air-gap:***

Air-gap is modeled with linear reluctance (Fig. 7). This reluctance is calculated from equation 1.

$$R_g = \frac{L_g}{\mu_0 A_g} \qquad (1)$$

Where $L_g$ is length of air-gap, $A_g$ is air-gap area and $\mu_0$ is magnetic permeability of free space ( $4\pi.10^{-7}$ ).


**Fig. 7 Modeling of Air-Gap**

***D. Flux leakage between two poles:***

Flux leakage is modeled with linear reluctance (Fig. 8).

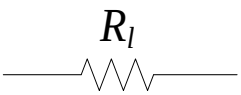


**Fig. 8 Modeling of Flux Leakage Between Two Poles**

## III. INTEGRATED MAGNETIC MODEL

This section offer a magnetic model for each of the six statuses that have been introduced in fig. 1.

**Status A:**

Fig. 3 shows the flux path in this status. With regard to the flux path in fig. 3, four independent areas can assume (regardless of flux between areas). These four areas are shown in fig. 9. The aim of this section is presented magnetic model for each of these four areas. Fig. 10 shows the winding energizing sequence with respect to fig. 1.

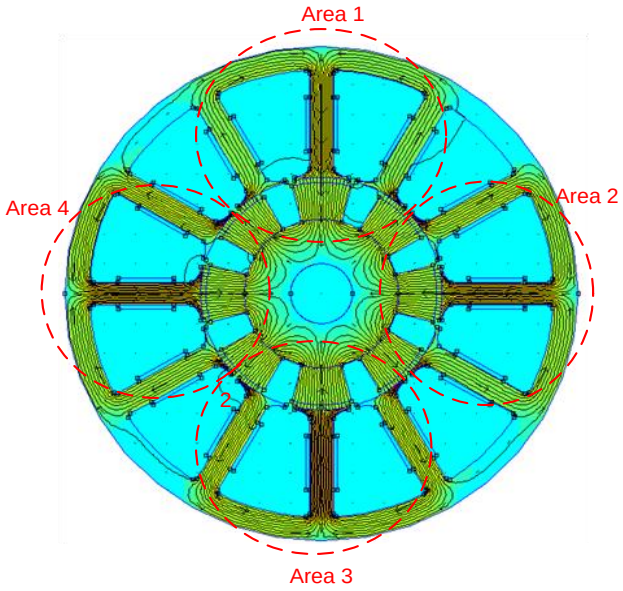


**Fig. 9 Flux Path and Four Areas in Status A**

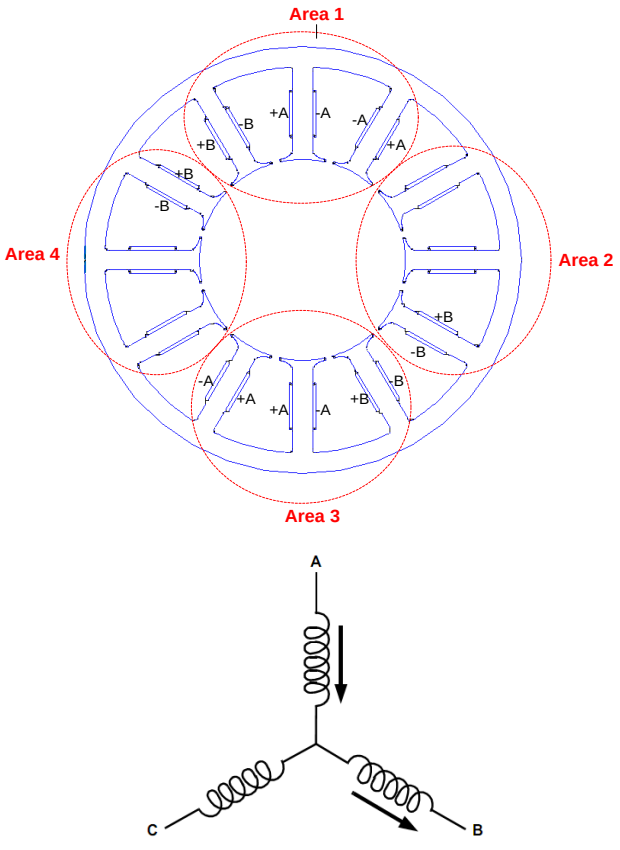


**Fig. 10 Winding Energizing Sequence in Status A**

Figures 11 to 14 are show the magnetic model for each of the four areas in status A.



*Published By:*
*Blue Eyes Intelligence Engineering*
*& Sciences Publication Pvt. Ltd.*

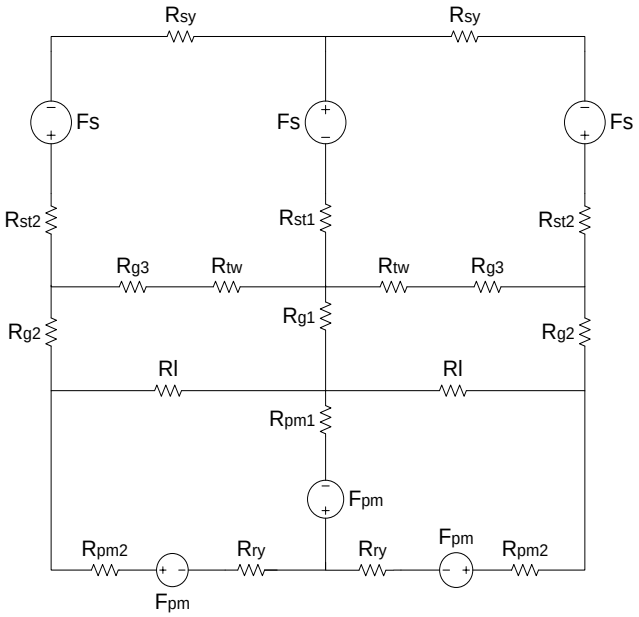


**Fig. 11 Magnetic Model for Area 1 in Status A**

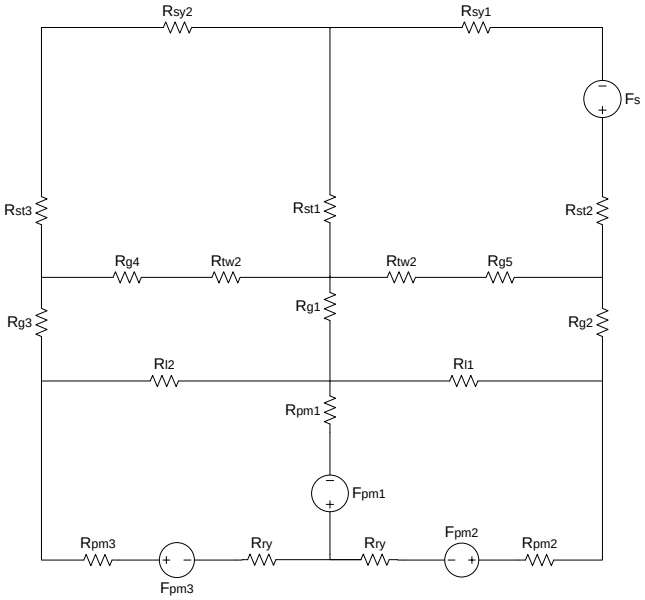


**Fig. 12 Magnetic Model for Area 2 in Status A**

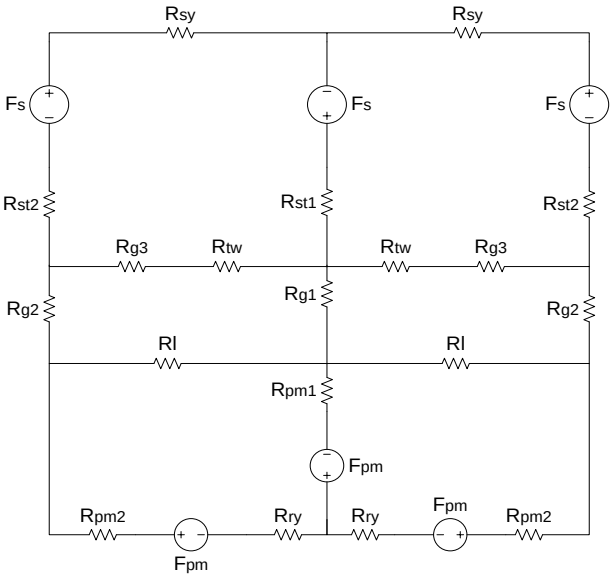


**Fig. 13 Magnetic Model for Area 3 in Status A**

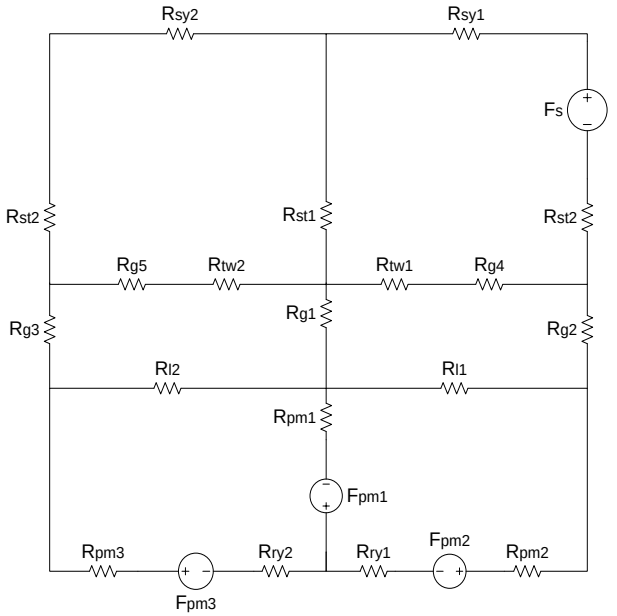


**Fig. 14 Magnetic Model for Area 4 in Status A**

Fig. 15 shows the algorithm for the analysis of the proposed magnetic models [4].

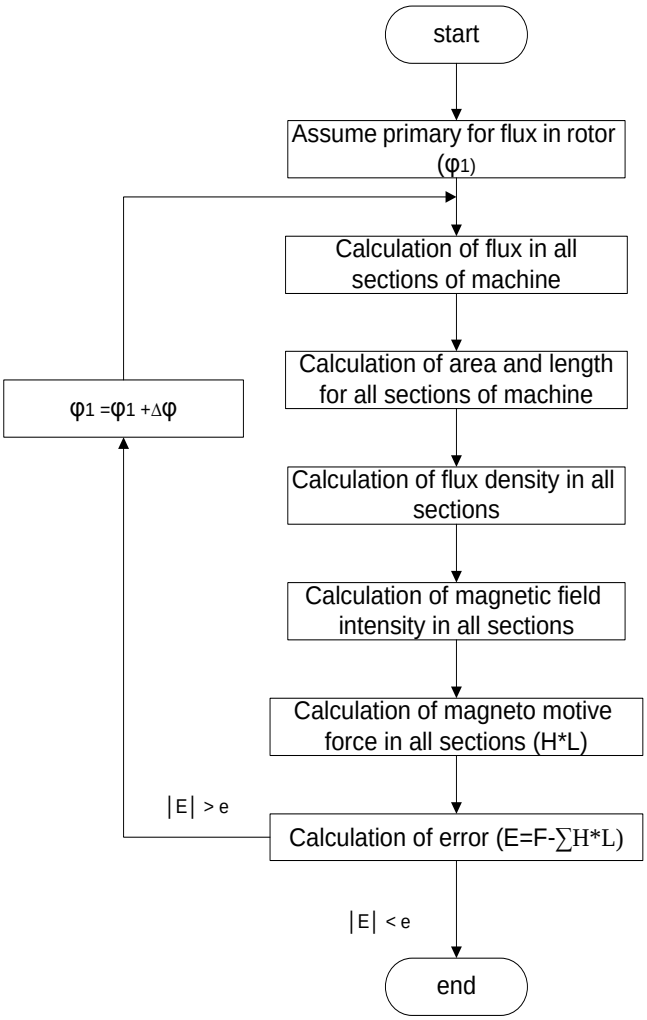


**Fig. 15 Flow Chart for the Evaluation of Machine Inductance**

The Comparison of analytical values and FEM simulation for each of the four magnetic models in status A are shown in Tables 2 to 5.



*Published By:*
*Blue Eyes Intelligence Engineering*
*& Sciences Publication Pvt. Ltd.*

**Table 2 Comparison of Analytical Value and FEM Simulation for Area 1**

| | FEM simulation | Analysis of magnetic model |
|---|---|---|
| Flux density in the air-gap (T) | 0.56 | 0.53 |
| Flux density in the stator yoke (T) | 0.55 | 0.57 |
| Flux density in the rotor yoke (T) | 0.6 | 0.56 |
| Flux density in the middle teeth (T) | 1.15 | 1.2 |

**Table 3 Comparison of Analytical Value and FEM Simulation for Area 2**

| | FEM simulation | Analysis of magnetic model |
|---|---|---|
| Flux density in the air-gap (T) | 0.58 | 0.55 |
| Flux density in the stator yoke (T) | 0.62 | 0.67 |
| Flux density in the rotor yoke (T) | 0.58 | 0.56 |
| Flux density in the middle teeth 1 (T) | 0.67 | 0.68 |
| Flux density in the middle teeth 2 (T) | 1.28 | 1.37 |
| Flux density in the middle teeth 3 (T) | 0.55 | 0.61 |

**Table 4 Comparison of Analytical Value and FEM Simulation for Area 3**

| | FEM simulation | Analysis of magnetic model |
|---|---|---|
| Flux density in the air-gap (T) | 0.61 | 0.58 |
| Flux density in the stator yoke (T) | 0.75 | 0.68 |
| Flux density in the rotor yoke (T) | 0.6 | 0.56 |
| Flux density in the middle teeth (T) | 1.48 | 1.42 |

**Table 5 Comparison of Analytical Value and FEM Simulation for Area 4**

| | FEM simulation | Analysis of magnetic model |
|---|---|---|
| Flux density in the air-gap (T) | 0.58 | 0.56 |
| Flux density in the stator yoke (T) | 0.68 | 0.68 |
| Flux density in the rotor yoke (T) | 0.6 | 0.56 |
| Flux density in the middle teeth 1 (T) | 0.76 | 0.73 |
| Flux density in the middle teeth 2 (T) | 1.34 | 1.3 |
| Flux density in the middle teeth 3 (T) | 0.63 | 0.65 |

Teeth 1, 2 and 3 for area 2 and 4 have been illustrated in fig.16.

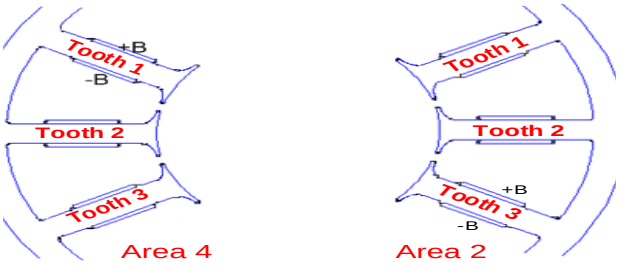


**Fig. 16 Illustration of Teeth in Area 2 and 4**

Tables 2 to 5 are shown that the proposed magnetic models are reasonably accurate.

**Status B:**

In this status the angle of rotor rotation is 15 degree. Fig. 17 shows the four areas in status B. Fig. 18 shows the winding energizing sequence with respect to the fig. 1.

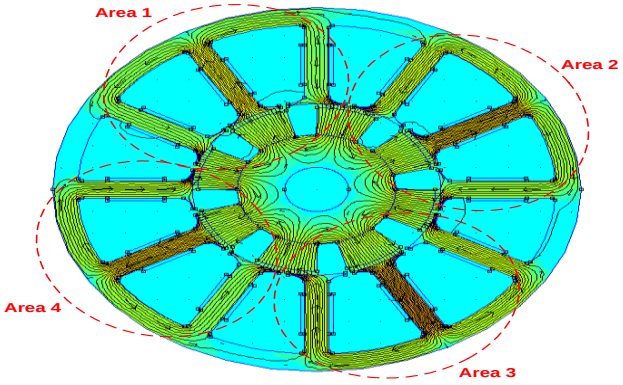


**Fig. 17 Flux Path and Four Areas in Status B**

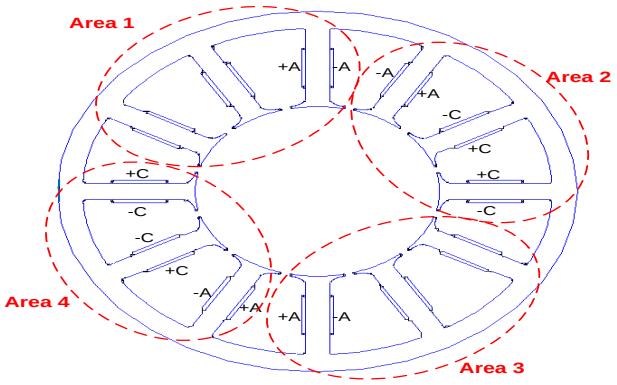


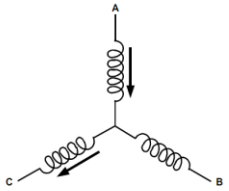


**Fig. 18 Winding Energizing Sequence in Status B**

Figures 19 to 22 are show the magnetic model for each of the four areas in status B.

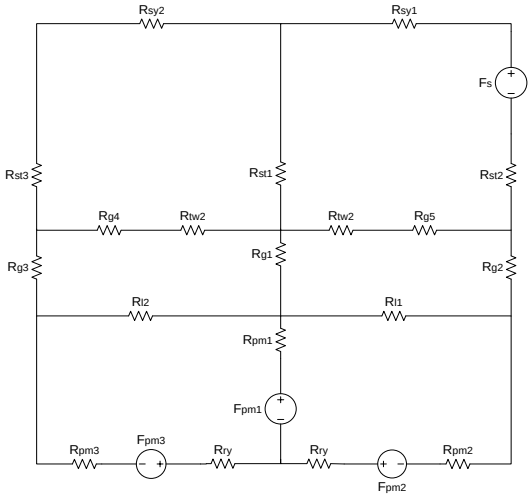


**Fig. 19 Magnetic Model for Area 1 in Status B**



*Published By:*
*Blue Eyes Intelligence Engineering*
*& Sciences Publication Pvt. Ltd.*

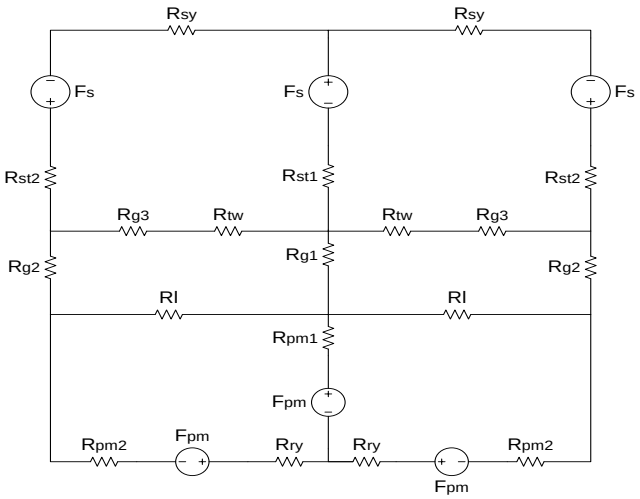


**Fig. 20 Magnetic Model for Area 2 in Status B**

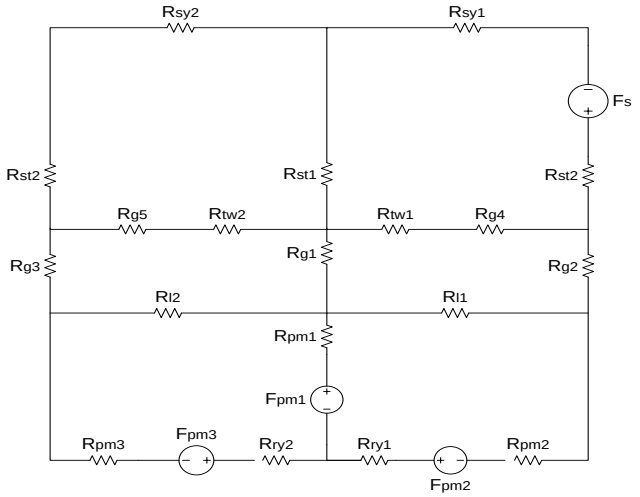


**Fig. 21 Magnetic Model for Area 3 in Status B**

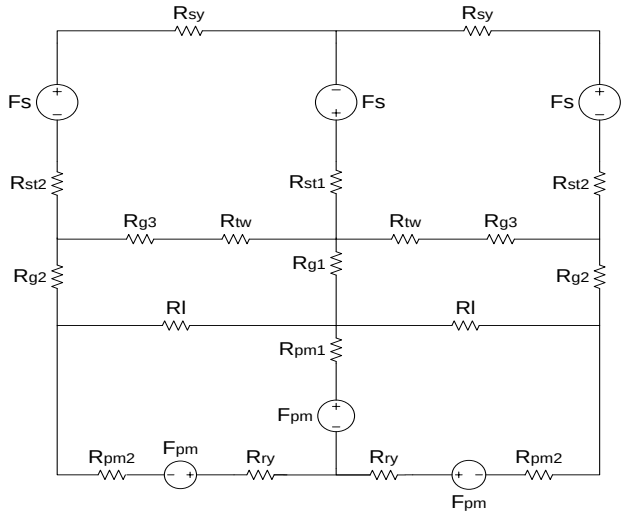


**Fig. 22 Magnetic Model for Area 4 in Status B**

Figures 12 and 19 are similar with the except that directions of flux passing are different. Thus in this status the results of table 3 can be used.

Figures 13 and 20 are similar with the except that directions of flux passing are different. Thus in this status the results of table 4 can be used.

Figures 14 and 21 are similar with the except that directions of flux passing are different. Thus in this status the results of table 5 can be used.

Figures 11 and 22 are similar with the except that directions of flux passing are different. Thus in this status the results of table 2 can be used.

**Status C:**

In this status the angle of rotor rotation is 30 degree. Fig. 23 shows the four areas in status C. Fig. 24 shows the winding energizing sequence with respect to the fig. 1.

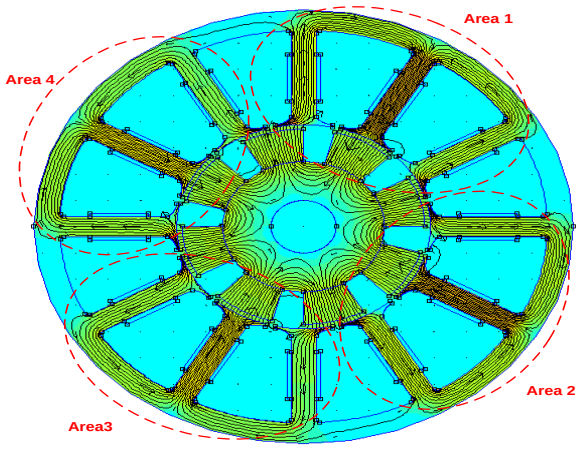


**Fig. 23 Flux Path and Four Areas in Status C**

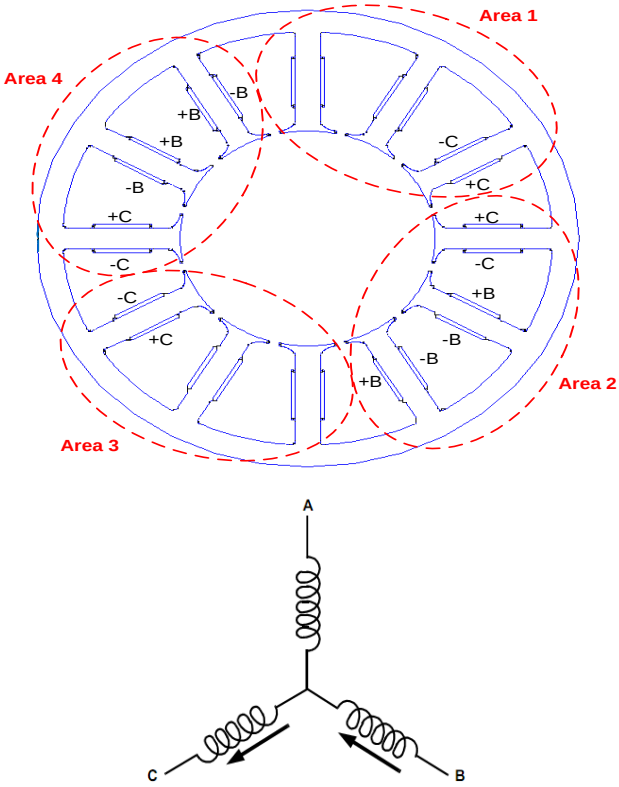


**Fig. 24 Winding Energizing Sequence in Status C**

There are many similarities between status A and C:

Area 1 in status C and area 4 in status A are similar. In this status the results of table 5 can be used.

Area 2 in status C and area 1 in status A are similar. In this status the results of table 2 can be used.

Area 3 in status C and area 2 in status A are similar. In this status the results of table 3 can be used.

Area 4 in status C and area 3 in status A are similar. In this status the results of table 4 can be used.



*Published By:*
*Blue Eyes Intelligence Engineering*
*& Sciences Publication Pvt. Ltd.*

**Status D:**

In this status the angle of rotor rotation is 45 degree. Fig. 25 shows the four areas in status D. Fig. 26 shows the winding energizing sequence with respect to the fig. 1.

There are many similarities between status D and B :

Area 1 in status D and area 4 in status B are similar. In this status the results of table 2 can be used.

Area 2 in status D and area 1 in status B are similar. In this status the results of table 3 can be used.

Area 3 in status D and area 2 in status B are similar. In this status the results of table 4 can be used.

Area 4 in status D and area 3 in status B are similar. In this status the results of table 5 can be used.

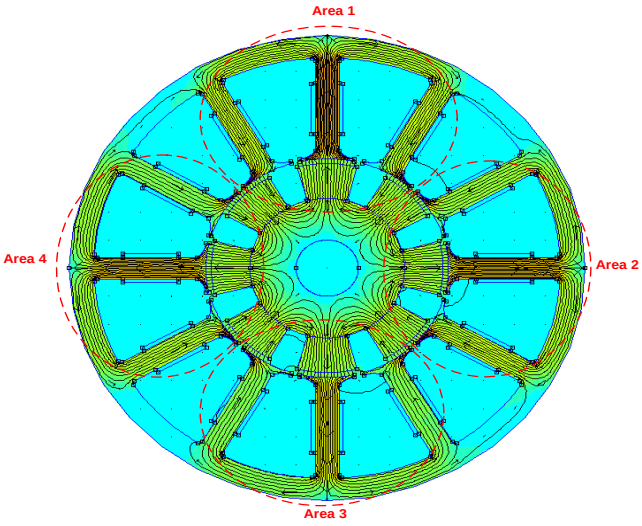


**Fig. 25 Flux Path and Four Areas in Status D**

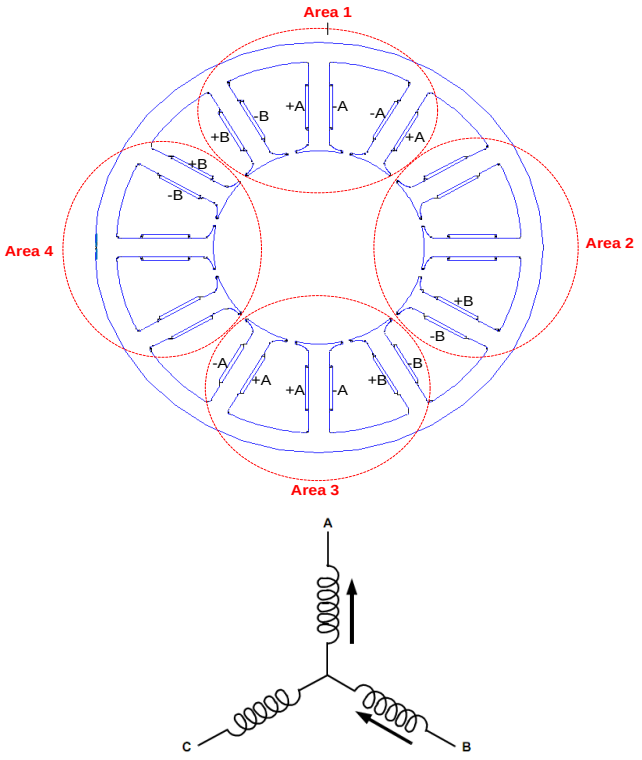


**Fig. 26 Winding Energizing Sequence in Status D**

**Status E:**

In this status the angle of rotor rotation is 60 degree. Fig. 27 shows the four areas in status E. Fig. 28 shows the winding energizing sequence with respect to the fig. 1.

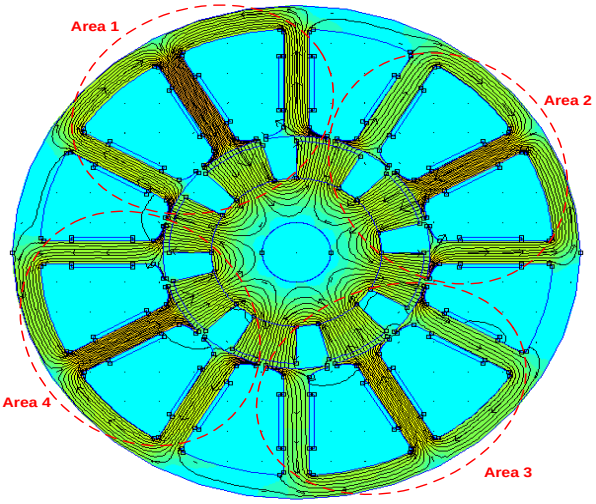


**Fig. 27 Flux Path and Four Areas in Status E**

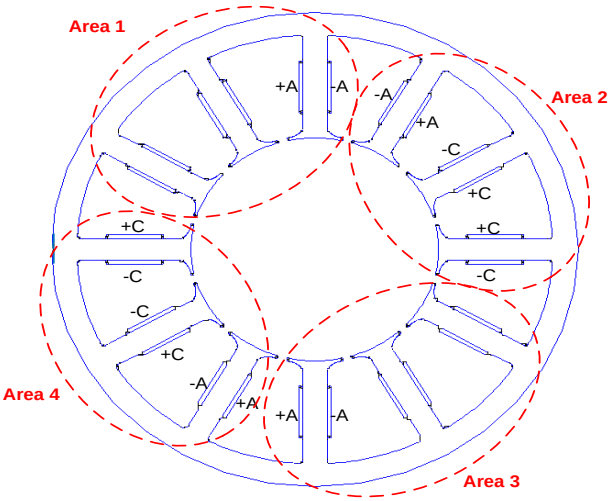


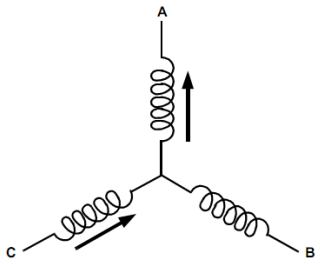


**Fig. 28 Winding Energizing Sequence in Status E**

There are many similarities between status E and A :

Area 1 in status E and area 2 in status A are similar. In this status the results of table 3 can be used.

Area 2 in status E and area 3 in status A are similar. In this status the results of table 4 can be used.

Area 3 in status E and area 4 in status A are similar. In this status the results of table 5 can be used.

Area 4 in status E and area 1 in status A are similar. In this status the results of table 2 can be used.

**Status F:**

In this status the angle of rotor rotation is 75 degree. Fig. 29 shows the four areas in status F. Fig. 30 shows the winding energizing sequence with respect to the fig. 1.



*Published By:*
*Blue Eyes Intelligence Engineering*
*& Sciences Publication Pvt. Ltd.*

There are many similarities between status F and B:
Area 1 in status F and area 3 in status B are similar. In this status the results of table 5 can be used.
Area 2 in status F and area 1 in status B are similar. In this status the results of table 3 can be used.
Area 3 in status F and area 4 in status B are similar. In this status the results of table 2 can be used.
Area 4 in status F and area 2 in status B are similar. In this status the results of table 4 can be used.

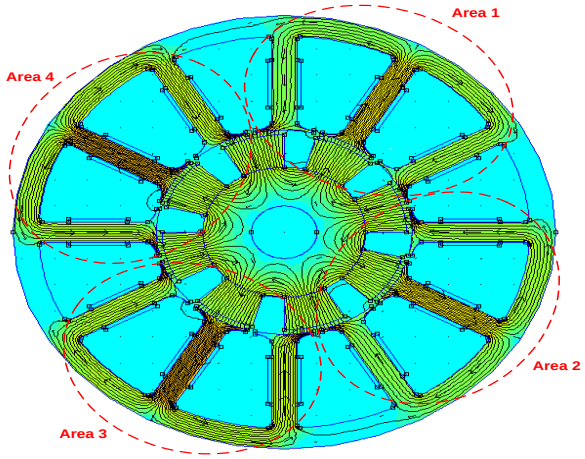


**Fig. 29 Flux Path and Four Areas in Status F**

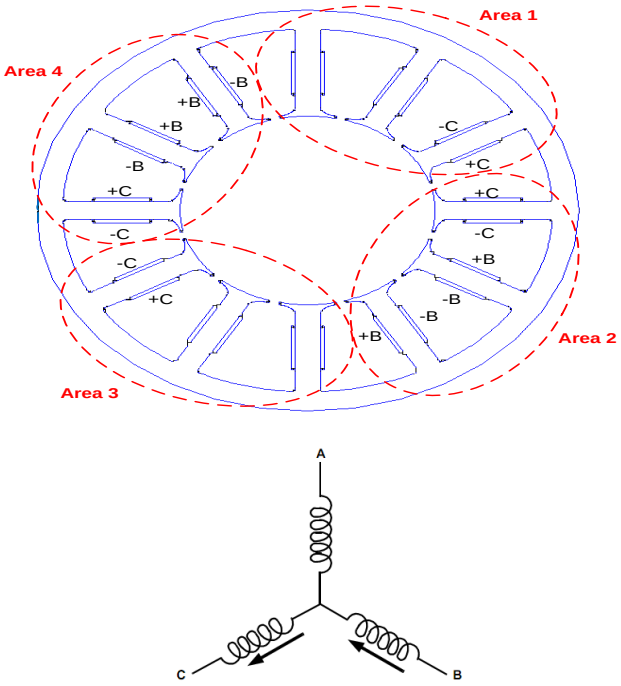


**Fig. 30 Winding Energizing Sequence in Status F**

## IV. Conclusion

Magnetic model is presented for radial flux surface mounted permanent magnet machine. Some advantages of proposed model are : Considering the effect of rotation in magnetic model, considering the leakage flux between two poles, cover all parts of the machine. Comparison of the analytical values with FEM simulations shows that the proposed magnetic models are reasonably accurate.

## V. Acknowledgment

The preferred spelling of the word “acknowledgment” in American English is without an “e” after the “g.” Use the singular heading even if you have many acknowledgments. Avoid expressions such as “One of us (S.B.A.) would like to thank” Instead, write “F. A. Author thanks” **Sponsor and financial support acknowledgments are placed in the unnumbered footnote on the first page**.

## References

[1] Jabbari, Ali, M. Shakeri, A. S. Gholamian, 2009. Rotor pole shape optimization of permanent magnet brushless DC motor using the reduced basis technique. Advances in electrical and computer engineering, 9: 75-81.
[2] Hassanpour Isfahani, Arash, and Sadeghi, Siavash, 2008. Design of a Permanent Magnet Synchronous Machine for the Hybrid Electric Vehicle. World Academy of Science, Engineering and Technology 45: 566-570.
[3] Meessen, K. J., Thelin, P., Soulard, J. and Lomonova1, E. A., 2008. Inductance Calculations of Permanent-Magnet Synchronous Machines Including Flux Change and Self- and Cross-Saturations. IEEE Transaction on magnetic, 44: 2324-2331.
[4] Krishnan, R., 2001. Switched Reluctance Motor Drives: Modeling, Simulation, Analysis, Design and Applications. 1st Edn. CRC Press, New York. ISBN-13: 978-0849308383, pp: 432.
[5] Sadeghierad, M., H. Lesani, H. Monsef and A. Darabi, 2008. Leakage in modeling of high speed axial flux PM generator. Proceedings of the IEEE International Conference on Industrial Technology, April 21-24, Chengdu, pp: 1–6.

**Payam Vahedi**, was born in Shahrekord, Iran, in 1985. He received the B.Sc. degree in electrical engineering from Chamran University, Ahvaz, Iran, in 2008 and M.Sc. degree in electrical engineering at Shahed University in 2010. He is now pursuing the phd degree in electrical engineering at Kashan University. His research activities are mostly on design and modeling of electrical machines.



*Published By:*
*Blue Eyes Intelligence Engineering*
*& Sciences Publication Pvt. Ltd.*